JOURNAL OF NATURAL PRODUCTS

pubs.acs.org/jnp

Article

Stilbenes with Potent Protein Tyrosine Phosphatase-1B Inhibitory Activity from the Roots of *Polygonum multiflorum*

Thi-Thuy An Nguyen,[⊥] Manh Tuan Ha,[⊥] Se-Eun Park, Jae Sue Choi, Byung Sun Min,* and Jeong Ah Kim*

Cite This: https://dx.doi.org/10.1021/acs.jnatprod.9b00777

Read Online

ACCESS | Metrics & More | Article Recommendations | Supporting Information

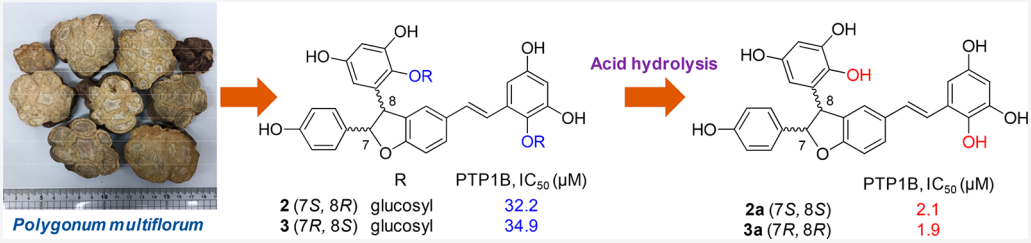

ABSTRACT: Seven new stilbene glycosides including three dimers (**1**−**3**) and four monomers (**4**−**7**) were isolated from the roots of *Polygonum multiflorum* along with nine previously identified stilbenes (**8**−**16**). In addition, two deglucosylated stilbenes, **2a** and **3a**, were also obtained as new dimeric stilbenes. The structures of the purified phytochemicals were elucidated by interpreting their spectroscopic data (NMR, HRMS, and ECD). To the best of our knowledge, this represents the first isolation of a phenylpropanoid (C_6−C_3) substituted with a stilbene unit (**7**) from the Polygonaceae family. In an in vitro enzyme assay with human recombinant protein tyrosine phosphatase-1B (PTP1B), compounds **2**−**5** showed weak PTP1B inhibition with an IC_{50} value range of 27.4−37.6 μM, while three deglucosylated stilbenes **2a**, **3a**, and **8a** exhibited IC_{50} values of 2.1, 1.9, and 12.1 μM, respectively. The inhibition modes and binding mechanism of selected inhibitors (**2a** and **3a**) were investigated using kinetic methods and molecular docking simulations.

Protein tyrosine phosphatase-1B (PTP1B), an intracellular nonreceptor member of the PTP superfamily, has emerged as a new drug target for therapeutic purposes in recent years. PTP1B plays a well-established role in down-regulating signaling in response to insulin and leptin.[1] In insulin signaling, PTP1B dephosphorylates activated insulin receptors and insulin receptor substrates to attenuate the cellular response to insulin binding.[1] In the leptin signaling pathway, PTP1B has the function of binding and dephosphorylation for Janus kinase 2, which is normally phosphorylated in response to leptin binding to the leptin receptor to trigger a feeling of satiety.[2] Knockout studies in mice have shown that PTP1B-deficient mice exhibit increased insulin sensitivity and obesity resistance.[3,4] These findings have motivated scientists to develop PTP1B inhibitors as potential therapies for diabetes and obesity.[1,5] Furthermore, recent findings have suggested that inhibiting PTP1B may have important applications in the treatment of cancer and inflammation.[6−9] In addition, PTP1B has recently emerged as a regulator of a variety of processes within the central nervous system, which may have implications in treating neurological disorders.[10−12] However, discovering selective PTP1B inhibitors with ideal pharmacological properties continues to be a challenge because of the low selectivity and the highly charged nature of the PTP1B catalytic domain.[13] Natural products have recently gained attention as novel PTP1B inhibitors, because they tend to be more efficacious in cells with high structural diversity when compared to synthetic compounds.[13]

Stilbenes, a class of plant phenols, have attracted biomedical interest for their intricate structures and diverse biological activities.[14,15] The structure of stilbenes is characterized by the presence of a 1,2-diphenylethylene nucleus; therefore, this class of compounds can be divided into two categories: monomeric and oligomeric stilbenes.[15] These subtypes are produced by coupling homogeneous or heterogeneous monomeric stilbenes with a variety of molecular skeletons. However, stilbenes are not widely distributed in plants, and phytochemical investigations have focused solely on a few families, including the Gnetaceae, Leguminosae, Polygonaceae, and Vitaceae.[15] Stilbene glycosides, the main active constituent in the rhizomes of *Polygonum multiflorum* Thunb. (Polygonaceae),[16] were reported to possess antioxidative,[17,18] anti-inflammatory,[19] and antiatherosclerotic activities.[20] *Polygonum multiflorum*, a Korean medicinal herb, has been historically used as an

Received: August 14, 2019

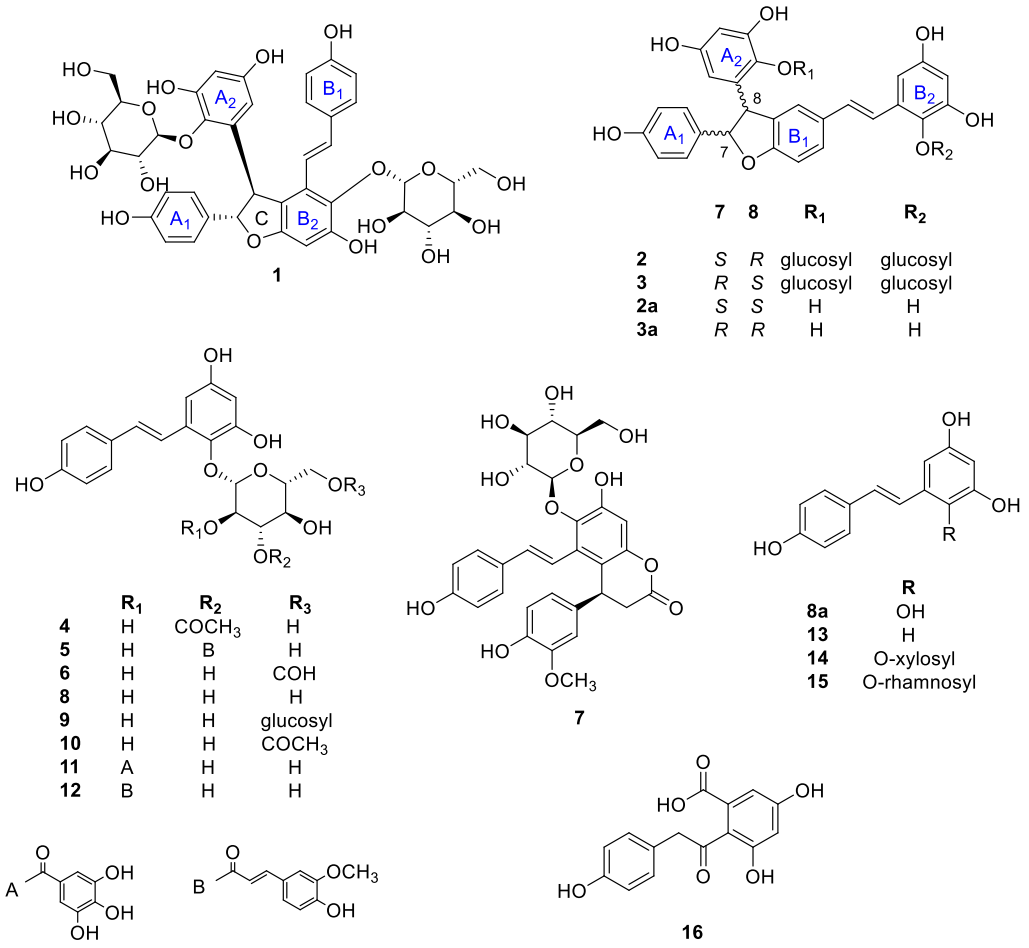

Figure 1. Chemical structures of compounds **1**−**16**, **2a**, **3a**, and **8a**.

antiallergy, antitumor, antibacterial, hemostatic, spasmolytic, and analgesic agent.[21] A previous study revealed that a MeOH extract of *P. multiflorum* inhibited PTP1B inhibitory activity with an IC_{50} value of 10.2 μg/mL.[22] However, there is currently no information regarding the PTP1B inhibitory activity of the chemical constituents of *P. multiflorum*. Thus, in the present study, the in vitro PTP1B inhibitory activity of 16 stilbenes including seven new stilbene glycosides isolated from *P. multiflorum* was investigated. Interestingly, three deglucosylated stilbenes (**2a**, **3a**, and **8a**) showed more potent PTP1B inhibition than their corresponding precursors (**2**, **3**, and **8**). In addition, enzyme kinetic analysis and molecular modeling were performed to characterize the interactions between the active stilbenes (**2a** and **3a**) and PTP1B, as well as their inhibitory mechanisms.

RESULTS AND DISCUSSION

A methanol extract of *P. multiflorum* roots was suspended in H_2O and successively partitioned with *n*-hexane, CH_2Cl_2, EtOAc, and *n*-BuOH. The EtOAc fraction (310.5 g) was separated by repeated column chromatography over silica gel, MCI gel, Sephadex LH-20, and semipreparative HPLC to afford seven new stilbene glycosides named polygonibenes A−G (**1**−**7**), along with nine known analogs (**8**−**16**) (Figure 1).

Polygonibene A (**1**) was obtained as a brown powder. Its molecular formula was established as $C_{40}H_{42}O_{18}$ by the HRFABMS sodium adduct molecular ion peak at *m*/*z* 833.2271 $[M + Na]^+$ (calcd for $C_{40}H_{42}O_{18}Na$, 833.2269). The UV spectrum of **1** showed absorption maxima at 310 and 235 nm. The IR spectrum of **1** exhibited absorption bands attributable to hydroxy (3322 cm^{-1}) and aromatic (1510 cm^{-1}) residues. The ^1H NMR data of **1** (Table 1) revealed the typical signals of a *trans*-disubstituted double bond [δ_H 7.33 (1H, d, J = 16.8 Hz, H-8′) and 6.85 (1H, d, J = 16.8 Hz, H-7′)], two *para*-disubstituted benzene rings [δ_H 7.28 (2H, d, J = 8.5 Hz, H-2,6) and 6.78 (2H, d, J = 8.5 Hz, H-3,5) for ring A_1 and 7.33 (2H, d, J = 8.5 Hz, H-2′,6′) and 6.72 (2H, d, J = 8.5 Hz, H-3′,5′) for ring B_1], a *meta*-tetrasubstituted benzene ring [δ_H 6.25 (1H, d, J = 2.9 Hz, H-12) and 5.89 (1H, d, J = 2.9 Hz, H-14) for ring A_2], a pentasubstituted benzene ring [δ_H 6.39 (1H, s, H-12′) for ring B_2], and two aliphatic proton signals [δ_H 5.52 (1H, d, J = 3.1 Hz, H-8) and 5.40 (1H, d, J = 3.1 Hz, H-7)]. In addition, signals corresponding to two anomeric protons [δ_H 4.60 (2H, d, J = 8.0 Hz)] were also evident in the ^1H NMR spectrum. The ^{13}C NMR and DEPT spectra of **1** showed the presence of 40 carbon signals that could be classified into 24 aromatic carbons, two olefinic carbons, two methine carbons, and 12 carbons of two sugar moieties. Through acid hydrolysis and subsequent TLC analysis of the monosaccharide derivative, the sugar units of **1** were identified as D-glucose. The D-glucose moieties were suggested to be the β-configuration due to the large $^3J_{1,2}$ value of the anomeric protons. The analysis of the above spectroscopic data, combined with the molecular formula, suggested that **1** is a dimeric stilbene glucoside consisting of

https://dx.doi.org/10.1021/acs.jnatprod.9b00777
J. Nat. Prod. XXXX, XXX, XXX−XXX

Table 1. ^{1}H NMR (500 MHz) and ^{13}C NMR (125 MHz) Data of Polygonibenes A−C (1−3) in Methanol-d_4

	1		2		3	
position	δ_C	δ_H, mult. (J in Hz)	δ_C	δ_H, mult. (J in Hz)	δ_C	δ_H, mult. (J in Hz)
1	134.2		133.9		132.8	
2	128.7	7.28, d (8.5)	128.7	7.27, d (8.6)	129.2	7.27, d (8.6)
3	116.2	6.78, d (8.5)	116.2	6.79, d (8.6)	116.1	6.78, d (8.5)
4	158.5		158.6		158.5	
5	116.2	6.78, d (8.5)	116.2	6.79, d (8.6)	116.1	6.78, d (8.5)
6	128.7	7.28, d (8.5)	128.7	7.27, d (8.6)	129.2	7.27, d (8.6)
7	93.9	5.40, d (3.1)	93.7	5.64, d (6.5)	95.0	5.47, d (7.8)
8	49.5	5.52, d (3.1)	49.6	5.56, d (6.5)	50.4	5.51, d (7.8)
9	139.8		133.3		133.3	
10	137.3		138.3		138.6	
11	151.6		151.6		151.7	
12	103.6	6.25, d (2.9)	103.7	6.29, d (2.9)	103.5	6.29, d (2.9)
13	156.2		156.3		156.3	
14	106.5	5.89, d (2.9)	106.3	6.18, d (2.9)	106.9	6.08, d (2.9)
1′	131.1		132.6		132.7	
2′	129.4	7.33, d (8.5)	124.2	7.30, d (1.5)	125.1	7.26, d (1.5)
3′	116.3	6.72, d (8.5)	138.8		138.3	
4′	158.3		160.6		161.0	
5′	116.3	6.72, d (8.5)	110.3	6.85, d (8.3)	110.1	6.85, d (8.3)
6′	129.4	7.33, d (8.5)	129.0	7.42, dd (8.3, 1.5)	128.5	7.48, dd (8.3, 1.5)
7′	134.6	6.85, d (16.8)	130.3	6.95, d (16.5)	130.3	6.94, d (16.4)
8′	121.0	7.33, d (16.8)	121.9	7.64, d (16.5)	122.4	7.67, d (16.4)
9′	131.1		133.6		133.8	
10′	138.9		137.8		137.9	
11′	152.1		152.1		152.0	
12′	97.8	6.39, s	103.7	6.26, d (2.8)	103.6	6.25, d (2.8)
13′	159.1		156.0		155.9	
14′	119.2		102.8	6.61, d (2.8)	102.8	6.59, d (2.8)
Glc1-1″	107.1	4.60, d (8.0)	107.8	4.64, d (7.0)	107.7	4.34, d (7.5)
2″	75.5	3.40[a]	75.5	3.43[a]	75.4	3.39[a]
3″	78.0	3.32, m	77.9	3.44[a]	77.8	3.38[a]
4″	70.6	3.40[a]	70.9	3.47[a]	71.0	3.38[a]
5″	78.2	2.89, m	78.2	3.25, m	78.2	3.21, m
6″	61.8	3.39, dd (12.0, 2.5)	62.3	3.75, dd (12.0, 2.5)	62.3	3.70, dd (12.0, 2.0)
		3.48 (12.0, 4.5)		3.66, dd (12.0, 4.5)		3.62, dd (12.0, 4.5)
Glc2-1‴	107.8	4.60, d (8.0)	108.0	4.50, d (7.9)	108.1	4.49, d (7.9)
2‴	75.5	3.56, m	75.5	3.56, m	75.4	3.53, m
3‴	77.9	3.43, m	77.9	3.44[a]	78.0	3.40[a]
4‴	70.9	3.51, t (7.5)	70.6	3.47[a]	70.9	3.48, m
5‴	78.2	3.27, m	78.3	3.19, m	78.2	3.27, m
6‴	62.1	3.76, dd (12.0, 2.5)	81.8	3.44[a]	62.3	3.79, dd (12.0, 2.5)
		3.70, dd (12.0, 4.5)		3.58, dd (12.0, 4.5)		3.68, dd (12.0, 4.5)

[a]Overlapped.

two (*E*)-2,3,5,4′-tetrahydroxystilbene-2-*O*-*β*-D-glucoside units connected together through a dihydrofuran bridge (C ring) to form a dimeric stilbene skeleton, which is common in natural oligomeric stilbenes.[23] The NMR data of **1** (Table 1) and *ε*-viniferin were similar,[23] except for the absence of two protons at positions 10 and 10′ as well as the appearance of two D-glucose moieties in **1**. This suggested that **1** resulted from the replacement of two protons at positions 10 and 10′ in *ε*-viniferin by two *O*-D-glucosyl groups, respectively. This inference was confirmed by the HMBC correlations (Figure 2) from H-1″ (Glc1, δ_H 4.60) to C-10 (δ_C 137.3) and H-1‴ (Glc2, δ_H 4.60) to C-10′ (δ_C 138.9). In addition, the *ε*-viniferin skeleton in **1** was further supported by the HMBC correlations (Figure 2) from H-7 (δ_H 5.40) to C-14′ (δ_C 119.2)/C-2 (δ_C 128.7), H-8 (δ_H 5.52) to C-13′ (δ_C 159.1)/C-10 (δ_C 137.3)/C-14 (δ_C 106.5), H-7′ (δ_H 6.85) to C-2′ (δ_C 129.4), and H-8′ (δ_H 7.33) to C-10′ (δ_C 138.9)/C-14′ (δ_C 119.2). The *trans* orientation of H-7 and H-8 in the furan ring was confirmed by the NOESY correlations (Figure 2) between H-7 (δ_H 5.40) and H-14 (δ_H 5.89) and between H-8 (δ_H 5.52) and H-2 (δ_H 7.28). The absolute configurations of the dihydrobenzofuran skeleton in **1** at C-7 and C-8 were determined via ECD data, which were examined in the range 220−240 nm.[24,25] The ECD spectrum of **1** showed a positive Cotton effect at 239 nm, opposite to that of (−)-*ε*-viniferin (7*R*,8*R*) (Figure S8.1, Supporting Information), indicating that the absolute configurations of **1** at C-7 and C-8 are 7*S* and 8*S*.[24,25] Thus, the structure of **1** was assigned as shown as a new dimeric stilbene glycoside (Figure 1) and was named polygonibene A.

https://dx.doi.org/10.1021/acs.jnatprod.9b00777
J. Nat. Prod. XXXX, XXX, XXX−XXX

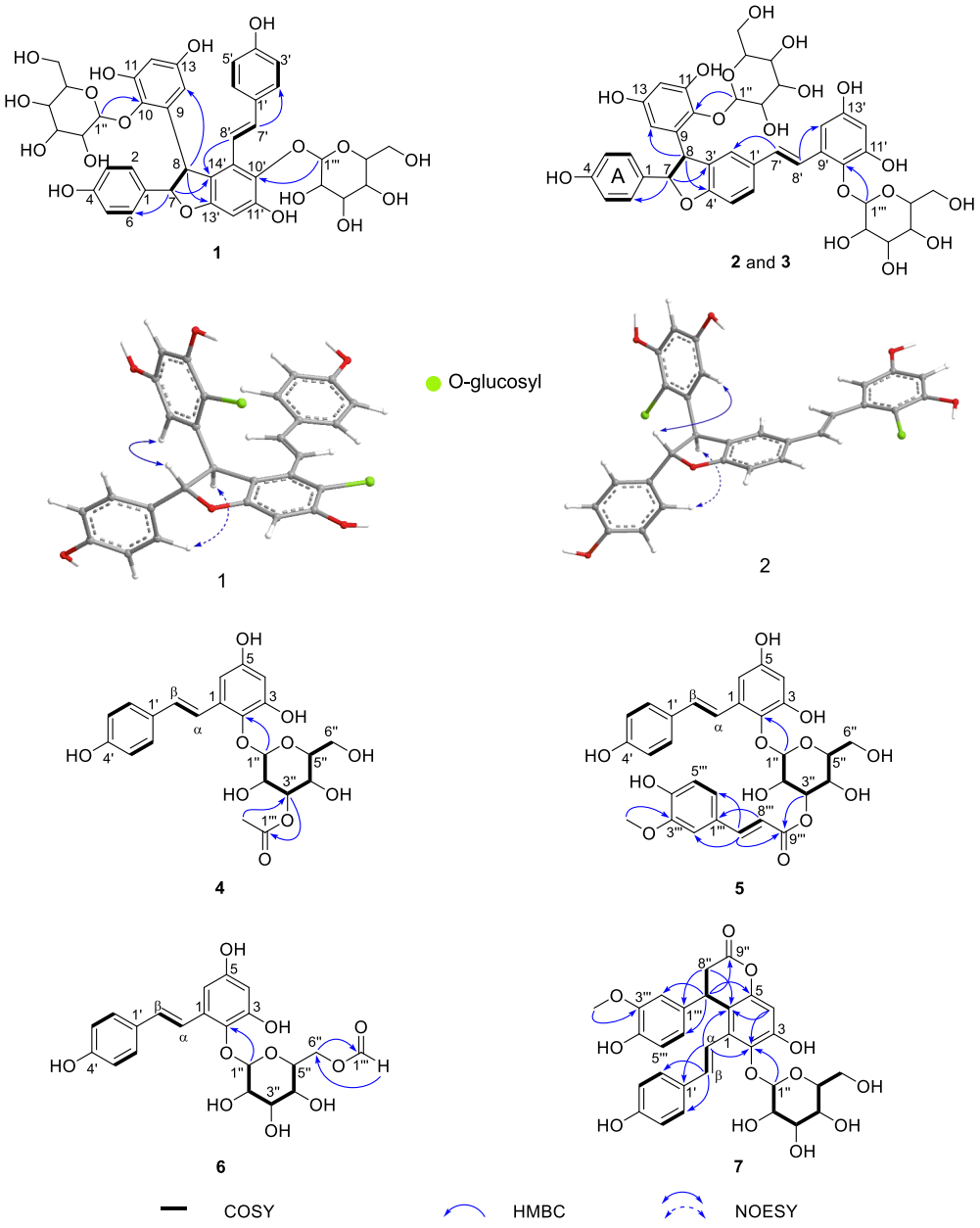

Figure 2. Key COSY, HMBC, and NOESY correlations of polygonibenes **1**−**7**.

A molecular formula of $C_{40}H_{42}O_{18}$ was established for polygonibene B (**2**, a brown powder with a positive optical rotation) based on the sodium adduct molecular ion peak at *m*/*z* 833.2273 $[M + Na]^+$ (calcd for $C_{40}H_{42}O_{18}Na$, 833.2269) in the HRFABMS. Similar to **1**, the ^{1}H NMR spectrum of **2** also revealed the presence of a *trans*-disubstituted double bond [δ_H 7.64 (1H, d, *J* = 16.5 Hz, H-8′) and 6.95 (1H, d, *J* = 16.5 Hz, H-7′)], a *para*-disubstituted benzene ring [δ_H 7.27 (2H, d, *J* = 8.6 Hz, H-2,6) and 6.79 (2H, d, *J* = 8.6 Hz, H-3,5)] for ring A_1, a *meta*-tetrasubstituted benzene ring [δ_H 6.29 (1H, d, *J* = 2.9 Hz, H-12) and 6.18 (1H, d, *J* = 2.9 Hz, H-14)] for ring A_2, two aliphatic protons [δ_H 5.64 (1H, d, *J* = 6.5 Hz, H-7) and 5.56 (1H, d, *J* = 6.5 Hz, H-8)], and two anomeric protons [δ_H 4.64 (1H, d, *J* = 7.0 Hz, H-1″) and 4.50 (1H, d, *J* = 7.9 Hz, H-1‴)]. In addition, the remaining aromatic proton signals belonged to an ABX coupling system [δ_H 7.30 (1H, d, *J* = 1.5 Hz, H-2′), 6.85 (2H, d, *J* = 8.3 Hz, H-5′), and 7.42 (1H, dd, *J* = 8.3, 1.5 Hz, H-6′)] for ring B_1 and an AX coupling system [δ_H 6.61 (1H, d, *J* = 2.8 Hz, H-14′) and 6.26 (1H, d, *J* = 2.8 Hz, H-12′)] for ring B_2. The ^{13}C NMR and DEPT spectra of **2** showed the presence of 40 carbon signals including 24 aromatic carbons, two olefinic carbons, two sp^3 methine carbons, and 12 carbons of two D-glucopyranosyl moieties. By performing the same method as used for **1**, both of the sugar moieties in **2** were determined as *β*-D-glucose. Comparison of the NMR data of **2** (Table 1) with those of *δ*-viniferin[26] revealed their close structural similarities, except for the replacement of two protons at positions 10 and 10′ in *δ*-viniferin by *O*-D-glucose moieties in **2**. This observation was confirmed by the HMBC correlations (Figure 2) from H-1″ (Glc1, δ_H 4.64) to C-10 (δ_C 138.3) and H-1‴ (Glc2) (δ_H 4.50) to C-10′ (δ_C 137.8). Assignments of all ^{1}H and ^{13}C NMR signals were accomplished by interpreting HMQC and HMBC spectra. The relative configuration of **2** was defined via

https://dx.doi.org/10.1021/acs.jnatprod.9b00777
J. Nat. Prod. XXXX, XXX, XXX−XXX

Table 2. ^{1}H NMR (500 MHz) and ^{13}C NMR (125 MHz) Data of Polygonibenes D−G (4−7)

	4[a]		5[a]		6[a]		7[b]	
position	δ_C	δ_H, mult. (J in Hz)	δ_C	δ_H, mult. (J in Hz)	δ_C	δ_H, mult. (J in Hz)	δ_C	δ_H, mult. (J in Hz)
1	133.4		133.4		133.4		133.8	
2	137.6		137.6		137.9		142.0	
3	152.1		152.0		152.0		151.4	
4	103.5	6.29, d (2.8)	103.5	6.31, d (2.8)	103.5	6.29, d (2.8)	105.1	6.68, s
5	155.9		155.9		155.9		151.5	
6	102.3	6.68, d (2.8)	102.3	6.70, d (2.8)	102.2	6.67, d (2.8)	116.0	
1′	130.4		130.4		130.5		130.1	
2′	129.0	7.48, d (8.6)	129.0	7.49, d (8.6)	128.9	7.42, d (8.6)	129.1	7.18, d (8.6)
3′	116.3	6.82, d (8.6)	116.3	6.82, d (8.6)	116.4	6.80, d (8.6)	116.4	6.73, d (8.6)
4′	158.1		158.1		158.1		158.8	
5′	116.3	6.82, d (8.6)	116.3	6.82, d (8.6)	116.4	6.80, d (8.6)	116.4	6.73, d (8.6)
6′	129.0	7.48, d (8.6)	129.0	7.49, d (8.6)	128.9	7.42, d (8.6)	129.1	7.18, d (8.6)
α	121.7	7.76, d (16.5)	121.7	7.79, d (16.5)	121.9	7.74, d (16.5)	120.4	7.32, d (16.8)
β	129.7	6.97, d (16.5)	129.7	6.98, d (16.5)	129.6	6.95, d (16.5)	136.1	6.34, d (16.8)
1″	107.4	4.70, d (7.9)	107.5	4.75, d (7.9)	107.7	4.60, d (7.7)	107.8	4.60, d (7.9)
2″	73.6	3.77, m	73.7	3.86, m	75.4	3.63, m	75.4	3.53, m
3″	78.7	5.09, t (9.5)	78.8	5.22, t (9.4)	77.6	3.58, m	77.9	3.42, m
4″	69.0	3.77, m	69.2	3.86, m	70.9	3.55, m	70.8	3.48, m
5″	77.8	3.54, m	77.8	3.60, m	75.2	3.68, m	78.2	3.19, m
6″	62.0	3.87, dd (11.8, 2.7)	62.1	3.86, m	63.7	4.45, dd (12.0, 1.4)	61.9	3.57, m
		3.81, dd (11.8, 4.3)				4.38, dd (12.0, 5.5)		
1‴	171.0		127.5		161.9	8.08, s	135.4	
2‴	21.2	2.07, s	111.3	7.38, d (1.8)			111.9	6.77, d (2.0)
3‴			148.8				149.6	
4‴			150.2				146.9	
5‴			116.1	6.89, d (8.2)			116.8	6.79, d (8.2)
6‴			124.0	7.18, dd (8.2, 1.8)			120.6	6.53, dd (8.2, 2.0)
7‴			146.1	7.65, d (15.9)			40.1	4.53, dd (5.9, 1.9)
8‴			116.0	6.46, d (15.9)			39.8	3.01, dd (15.5, 6.2)
								2.91, dd (15.5, 2.1)
9‴			167.7				170.3	
OCH_3-3‴			56.4	3.94 (s)			56.4	3.80 (s)

[a]In acetone-d_6. [b]In methanol-d_4.

the NOESY spectrum. The NOESY correlations (Figure 2) between H-7 (δ_H 5.64) and H-14 (δ_H 6.18), as well as H-8 (δ_H 5.56) and H-2 (δ_H 7.27), revealed a *trans* relationship between H-7 and H-8. The absolute configurations of **2** at C-7 and C-8 were deduced from the absolute configuration of its deglucosylated stilbene (**2a**) via ECD data analysis. The ECD spectrum of **2a** displayed a positive Cotton effect at 239 nm that was opposite to that of (−)-*δ*-viniferin (7*R*,8*R*) (Figure S8.2, Supporting Information), indicating that the absolute configurations of **2a** are 7*S* and 8*S*.[24,25] Subsequently, the absolute configurations of **2** were determined as 7*S* and 8*R*. Thus, the structure of **2** (polygonibene B) was assigned as shown in Figure 1 and is a new dimeric stilbene glycoside.

Polygonibene C (**3**) was isolated as a brown powder with a negative optical rotation. The molecular formula of **3** was determined to be the same as **2** ($C_{40}H_{42}O_{18}$) based on the HRFABMS sodium adduct molecular ion peak at m/z 833.2272 $[M + Na]^+$ (calcd for $C_{40}H_{42}O_{18}Na$, 833.2269). Compounds **2** and **3** were obtained by HPLC chromatographic purification with different retention times under the same conditions [**2** (t_R = 27.0 min) and **3** (t_R = 32.0 min)]. The structural features of **3**, including 1D NMR and HMBC correlations, were similar to those of **2** (Table 1 and Figure 2). However, the optical rotation and ECD data of **3** differ from those of **2**, indicating that **3** is a stereoisomer of **2**. In addition, acid hydrolysis of **2** and **3** formed the aglycone compounds **2a** and **3a**, respectively. The ^{1}H NMR spectra of **2a** and **3a** (Experimental Section) were also similar, but their optical rotations and ECD data (Figure S8.2, Supporting Information) were opposite. This further supported that compounds **2** and **3** contain enantiomeric aglycones. The relative configuration of C-7/8 was determined to be *trans* according to the NOESY correlations (Figure 2) between H-7 (δ_H 5.47) and H-14 (δ_H 6.08), as well as H-8 (δ_H 5.51) and H-2 (δ_H 7.27). The **3a** ECD data were similar to those of (−)-*δ*-viniferin (7*R*,8*R*) (Figure S8.2, Supporting Information), indicating that **3a** and (−)-*δ*-viniferin have the same absolute configurations (7*R*,8*R*).[24,25] Consequently, the absolute configurations of **3** were determined as 7*R* and 8*S*. Based on the above analysis, the structure of **3**, a new dimeric stilbene glycoside (polygonibene C), was assigned as shown in Figure 1.

Polygonibene D (**4**) was isolated as a brown powder. The HRFABMS of **4** showed a protonated molecular ion peak at m/z 449.1445 $[M + H]^+$ (calcd for $C_{21}H_{25}O_{10}$, 449.1458), corresponding to the molecular formula $C_{21}H_{24}O_{10}$. Similar to **8**, the ^{1}H NMR spectrum of **4** also showed the typical signals of an (*E*)-2,3,5,4′-tetrahydroxystilbene-2-*O*-*β*-D-glucoside derivative, with a *trans*-disubstituted double bond at δ_H 7.76 (1H, d, J = 16.5 Hz, H-α) and 6.97 (1H, d, J = 16.5 Hz, H-β), two aromatic rings with one AABB coupling system at δ_H 7.48 (2H,

https://dx.doi.org/10.1021/acs.jnatprod.9b00777
J. Nat. Prod. XXXX, XXX, XXX−XXX

d, J = 8.6 Hz, H-2′,6′) and 6.82 (2H, d, J = 8.6 Hz, H-3′,5′), one AX coupling system at δ_H 6.68 (1H, d, J = 2.8 Hz, H-6) and δ_H 6.29 (1H, d, J = 2.8 Hz, H-4), and an anomeric proton at δ_H 4.70 (1H, d, J = 7.9 Hz, H-1″) (Table 2). In addition, the signals of an acetoxy group [δ_H 2.07 (3H, s); δ_C 171.0 (−OC═O), 21.2 (−CH_3)] were also observed in the 1D NMR spectra of **4**. The ^{13}C NMR spectrum of **4** in combination with DEPT analysis revealed the signals of 21 carbons that included one carbonyl carbon, eight sp^2, four sp^3 methines, one sp^3 methylene carbon, six quaternary carbons, and one methyl carbon. Inspection of the NMR data of **4** indicated that this compound is structurally quite similar to **8**, except for the replacement of a hydroxy group with an acetoxy group in the glucose moiety. The position of the acetoxy group at C-3″ was verified by the HMBC correlation between H-3″ (δ_H 5.09) and carbonyl carbon (δ_C 171.0) (Figure 2), as well as the downfield shift of C-3″ (δ_C 78.7) and the upfield shift of C-2″ (δ_C 73.6), in **4** compared with those of **8** [δ_C 77.5 (C-3″), 75.0 (C-2″)].[27] Therefore, the structure of **4** (polygonibene D) was elucidated as (*E*)-2,3,5,4′-tetrahydroxystilbene-2-*O*-(3″-*O*-acetyl)-*β*-D-glucoside, a new monomeric stilbene glycoside.

The HRESIMS of polygonibene E (**5**, a brown powder) exhibited a sodium adduct molecular ion peak at m/z 605.1636 $[M + Na]^+$ (calcd for $C_{30}H_{30}O_{12}Na$, 605.1635), corresponding to the molecular formula $C_{30}H_{30}O_{12}$. A comparison of the ^{1}H and ^{13}C NMR spectra of **5** with those of **4** indicated that the difference was only in the signals belonging to the substituent at C-3″ of the glucose moiety (Table 2). These signals were attributable to the replacement of the acetoxy group in **4** with a feruloyl group [δ_H 7.38 (1H, d, J = 1.8 Hz, H-2‴), 6.89 (1H, d, J = 8.2 Hz, H-5‴), 7.18 (1H, dd, J = 8.2, 1.8 Hz, H-6‴), 7.65 (1H, d, J = 15.9 Hz, H-7‴), 6.46 (1H, d, J = 15.9 Hz, H-8‴), and 3.94 (3H, s, OCH_3-3‴); δ_C 127.5 (C-1‴), 111.3 (C-2‴), 148.8 (C-3‴), 150.2 (C-4‴), 116.1 (C-5‴), 124.0 (C-6‴), 146.1 (C-7‴), 116.0 (C-8‴), 167.7 (C-9‴), and 56.4 (OCH_3-3‴)] in **5**.[28] This was confirmed by the HMBC correlations from H-7‴ to C-2‴/C-6‴/C-9‴, H-8‴ to C-1‴, H-3″ to C-9‴, and H-1″ to C-2 (Figure 2). Therefore, the structure of **5** (polygonibene E) was elucidated as (*E*)-2,3,5,4′-tetrahydroxystilbene-2-*O*-(3″-*O*-feruloyl)-*β*-D-glucoside, a new monomeric stilbene glycoside.

Polygonibene F (**6**) was obtained as a brown powder with the molecular formula $C_{21}H_{22}O_{10}$ based on the HRFABMS protonated molecular ion peak at m/z 435.1288 $[M + H]^+$ (calcd for $C_{21}H_{23}O_{10}$, 435.1291). The ^{1}H and ^{13}C NMR spectra of **6** (Table 2) were similar to those of **8** except for additional signals due to a formyl group (HCOO−) [δ_H 8.08 (1H, s); δ_C 161.9] in **6**.[29] The position of the attached formyl group at C-6″ was verified by the downfield shift of H_2-6″ (δ_H 4.45, 4.38) in **6** compared with those of **8** [δ_H 3.86 (H_2-6″)] and the HMBC correlations from δ_H 8.08 (1H, s, HCOO−) to δ_C 63.7 (C-6″) and δ_H 4.45/4.38 (H_2-6″) to δ_C 161.9 (HCOO−) (Figure 2). Thus, the structure of **6** (polygonibene F) was elucidated as (*E*)-2,3,5,4′-tetrahydroxystilbene-2-*O*-(6″-formyl)-*β*-D-glucoside, a new monomeric stilbene glycoside.

The molecular formula of polygonibene G (**7**, a brown powder) was determined to be $C_{30}H_{30}O_{12}$ based on its HRESIMS data [a sodium adduct molecular ion peak at m/z 605.1631 $[M + Na]^+$ (calcd for $C_{30}H_{30}O_{12}Na$, 605.1635)]. The ^{1}H NMR spectrum of **7** (Table 2) also showed proton signals of a stilbene glycoside: a *trans*-disubstituted double bond at δ_H 7.32 (1H, d, J = 16.8 Hz, H-*α*) and 6.34 (1H, d, J = 16.8 Hz, H-*β*), a *para*-disubstituted benzene ring at δ_H 7.18 (2H, d, J = 8.6 Hz, H-2′,6′) and 6.73 (2H, d, J = 8.6 Hz, H-3′,5′), a pentasubstituted benzene ring at δ_H 6.68 (1H, s, H-4), and an anomeric proton at δ_H 4.60 (1H, d, J = 7.9 Hz, H-1″). In addition, the proton signals of a trisubstituted benzene ring at δ_H 6.77 (1H, d, J = 2.0 Hz, H-2‴), 6.79 (1H, d, J = 8.2 Hz, H-5‴), and 6.53 (1H, dd, J = 8.2, 2.0 Hz, H-6‴), a methoxy group at δ_H 3.80 (3H, s, OCH_3-3‴), three aliphatic proton signals at δ_H 4.53 (1H, dd, J = 5.9, 1.9 Hz, H-7‴), 3.01 (1H, dd, J = 15.5, 6.2 Hz, H-8‴), and 2.91 (1H, d, J = 15.5, 2.1 Hz, H-8‴), and the carbon signal of a carbonyl group at δ_C 170.3 (C-9‴) suggested the presence of an aromatic 3-methoxy-4-hydroxy system substituted by a *δ*-lactone moiety, which was similar to the phenylpropanoid (C_6−C_3) moiety of gnetumontanins C−G.[30,31] The ^{13}C NMR and DEPT spectra of **7** (Table 2) revealed the presence of 30 carbon atoms including a carbonyl carbon, 10 sp^2 methines, 6 sp^3 methines, 2 sp^3 methylenes, 10 quaternary carbons, and one methoxy carbon. The *β*-linkage of the glucosyl moiety was deduced from the 7.9 Hz coupling constant of the anomeric proton signal at δ_H 4.60. The above data suggested that **7** is a stilbene glucoside consisting of an (*E*)-2,3,5,4′-tetrahydroxystilbene-2-*O*-*β*-D-glucoside unit and a ferulic acid unit connected together through a *δ*-lactone bridge. This was confirmed along with the location of the *δ*-lactone moiety by the HMBC correlations from H-7‴ (δ_H 4.53)/H_2-8‴ (δ_H 3.01, 2.91)/H-4 (δ_H 6.68)/H-*α* (δ_H 7.32) to C-6 (δ_C 116.0) and H-7‴ (δ_H 4.53)/H-4 (δ_H 6.68) to C-5 (δ_C 151.5) (Figure 2). The absolute configuration of **7** at C-7‴ was determined by analyzing the ECD data. In a previous study, the 7‴*S* configuration of the phenylpropanoid (C_6−C_3) moiety in apocynin B was characterized by a positive Cotton effect at 233 nm ([*θ*] +7590).[32] In the present investigation, the ECD spectrum of **7** exhibited a positive Cotton effect at 229 nm (+4.61), indicating that the absolute configuration of **7** at C-7‴ is also in the *S* form. Based on the above analysis, the structure of **7** (polygonibene G) was assigned as shown in Figure 1.

The nine known compounds were identified as (*E*)-2,3,5,4′-tetrahydroxystilbene-2-*O*-*β*-D-glucoside (**8**),[27] (*E*)-2,3,5,4′-tetrahydroxystilbene-2-*O*-(6″-*O*-*β*-D-glucopyranoside)-*β*-D-glucoside (**9**),[33] (*E*)-2,3,5,4′-tetrahydroxystilbene-2-*O*-(6″-*O*-acetyl)-*β*-D-glucoside (**10**),[21] (*E*)-2,3,5,4′-tetrahydroxystilbene-2-*O*-(2″-*O*-galloyl)-*β*-D-glucoside (**11**),[21] (*E*)-2,3,5,4′-tetrahydroxystilbene-2-*O*-(2″-*O*-feruloyl)-*β*-D-glucoside (**12**),[28] resveratrol (**13**),[34] (*E*)-2,3,5,4′-tetrahydroxystilbene-2-*O*-*β*-D-xyloside (**14**),[35] (*E*)-2,3,5,4′-tetrahydroxystilbene-2-*O*-*α*-L-rhamnoside (**15**), and 3,5-dihydroxy-2-[2-(4-hydroxyphenyl)acetyl]benzoic acid (**16**)[36] (Figure 1) based on the analysis of their observed and reported spectroscopic data. Herein, the ^{1}H and ^{13}C NMR data of compound **15** are established for the first time based on conventional NMR techniques (^{1}H−^{1}H COSY, HMQC, and HMBC).

The PTP1B inhibitory activity of the isolated compounds (**1**−**16**) and three deglucosylated stilbenes (**2a**, **3a**, and **8a**) were evaluated using *p*-nitrophenyl phosphate (*p*-NPP) as a substrate, and IC_{50} values were determined by linear regression analysis (Table 3). As a result, compounds **2**−**5**, **9**, and **13**, together with three aglycones (**2a**, **3a**, and **8a**), significantly inhibited PTP1B compared to the non-inhibitor-treated control group (p < 0.05). The other compounds did not show significant inhibition under the tested concentration (IC_{50} > 50 *μ*M). The new compounds (**2**−**5**) showed weak PTP1B inhibition with an IC_{50} range of 27.4−37.6 *μ*M, while

https://dx.doi.org/10.1021/acs.jnatprod.9b00777
J. Nat. Prod. XXXX, XXX, XXX−XXX

Table 3. Inhibitory Activity of Compounds 1−16, 2a, 3a, and 8a against PTP1B

compound	PTP1B inhibition, IC_{50}[a] (μM)	K_i value[b]	inhibition type[c]
1, 6−16	>50	[e]	[e]
2	32.2 ± 0.46	[e]	[e]
3	34.9 ± 0.58	[e]	[e]
4	37.6 ± 3.02	[e]	[e]
5	27.4 ± 0.02	[e]	[e]
8a	12.1 ± 0.53	[e]	[e]
2a	2.1 ± 0.08	1.02	noncompetitive
3a	1.9 ± 0.04	0.92	noncompetitive
sodium orthovanadate[d]	15.1 ± 1.76	[e]	[e]
ursolic acid[d]	5.0 ± 0.02	[e]	[e]

[a]The 50% inhibition concentrations (IC_{50}, μM) are expressed as the mean ± SEM four independent experiments. [b]Determined by Dixon plot. [c]Determined by Lineweaver−Burk plots. [d]Used as positive control. [e]Not tested.

the three deglucosylated stilbenes (**2a**, **3a**, and **8a**) exhibited more potent activity with IC_{50} values of 2.1, 1.9, and 12.1 μM, respectively. In comparison, the IC_{50} values of the positive controls (ursolic acid and sodium orthovanadate) were 5.0 and 15.1 μM, respectively. This suggested that the presence of glucose moieties negatively influences the resultant PTP1B inhibitory activity of stilbene glycosides. This finding is similar to a previous study, in which the deglucosylated stilbene **8a** exhibited much stronger DPPH radical scavenging activity (IC_{50} = 0.4 mM) compared to its corresponding precursor (**8**, IC_{50} = 40 mM).[18]

In addition, the structure−activity relationships for (*E*)-2,3,5,4′-tetrahydroxystilbene-2-*O*-β-D-glucoside derivatives (**4−6** and **9−12**) were also observed in the PTP1B inhibitory assay. Compounds **4** and **5**, in which the C-3″ of the glucose moiety was substituted, showed stronger inhibition than **6** and **9−12**, which have other substituent positions. This suggested that a substituent occurring at position C-3″ on the glucose moiety might positively influence the PTP1B inhibitory activity of (*E*)-2,3,5,4′-tetrahydroxystilbene-2-*O*-β-D-glucoside derivatives.

Since the aglycone stilbenes (**2a** and **3a**) showed the strongest PTP1B inhibition, the mode of inhibition and inhibition constants (K_i values) of these compounds were further investigated using two kinetic methods: Lineweaver−Burk and Dixon plots (Figure S9, Supporting Information). In the Lineweaver−Burk plot, the lines crossed at the same point on the *x*-intercept, and the *y*-intercept increased as the inhibitor concentration increased, indicating that both **2a** and **3a** inhibited PTP1B via noncompetitive mechanisms. The results of Dixon plots also indicated that PTP1B inhibition was noncompetitive for **2a** and **3a** (Figure S9, Supporting Information) with K_i values of 1.02 and 0.92 μM, respectively (Table 3).

To investigate the protein−ligand interaction geometries for compounds **2a** and **3a** at a molecular level, molecular docking simulation of these compounds and the reference ligands [compound B (an allosteric inhibitor) and ursolic acid (a catalytic inhibitor)] were performed using AutoDock 4.2 software. The molecular docking models of the deglucosylated stilbenes (**2a** and **3a**) are illustrated in Figure 3. The binding energies of **2a**, **3a**, ursolic acid, and compound B with interacting residues (H-bond and van der Waals interacting residues), along with the number of H-bonds, are listed in Table 4. In a previous study, three α helices [α3 helix (Glu186−Glu200), α6 helix (Ala264−Ile281), and α7 helix (Val287−Ser295)] were reported as core regions of the allosteric site in PTP1B.[37] The docking results presented here show that compound **2a** binds to the allosteric site of PTP1B with a binding energy of −7.01 kcal/mol by forming three

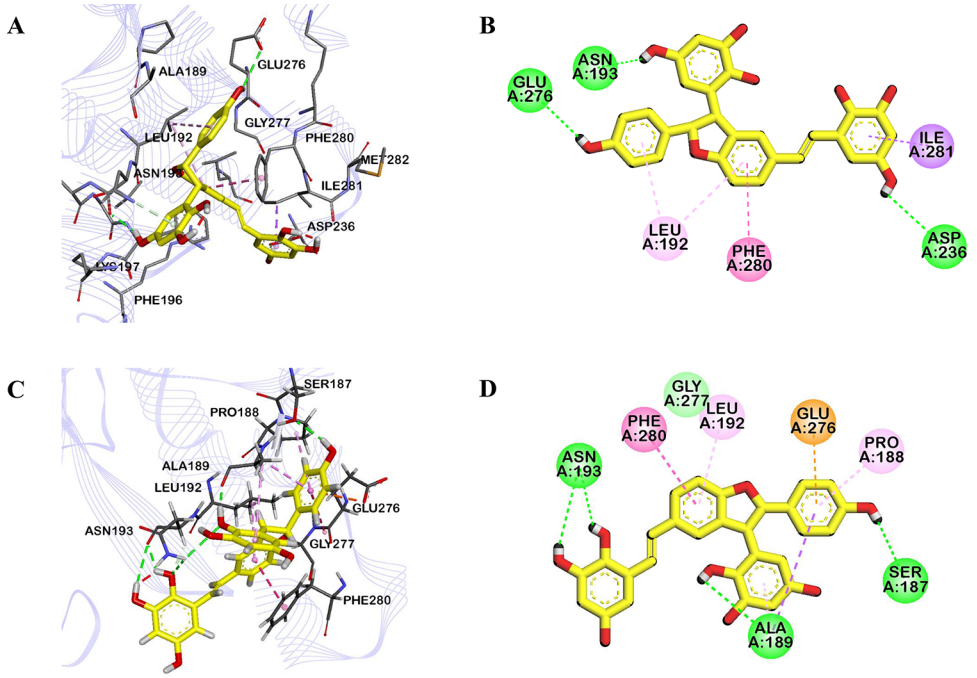

Figure 3. Inhibition mode of **2a** (A) and **3a** (C) for the PTP1B allosteric site and 2D ligand interaction diagram of PTP1B allosteric inhibition by **2a** (B) and **3a** (D).

https://dx.doi.org/10.1021/acs.jnatprod.9b00777
J. Nat. Prod. XXXX, XXX, XXX−XXX

Table 4. Binding Site Residues and Docking Scores of Compounds 2a, 3a, and Reported Inhibitors of PTP1B Obtained Using Autodock 4.2

compound	binding energy[a] (kcal/mol)	no. of H-bonds[b]	H-bond interacting residues[b]	van der Waals interacting residues[b]	hydrophobic interacting residues[b]	electrostatic interacting residues[b]
2a	−7.01	3	Asp236, Asn193, Glu276		Ile281 ($\pi-\delta$), Leu192 (π−alkyl), Phe280 ($\pi-\pi$ T-shaped)	
3a	−9.35	4	Asn193, Ala189, Ser187	Gly277	Phe280 ($\pi-\pi$ stacked), Leu192 Pro188 (π−alkyl), Ala189 (π−alkyl and $\pi-\sigma$)	Glu276 (π−anion)
ursolic acid (catalytic inhibitor)	−8.88	3	Arg24, Arg254		Tyr46, Arg24 (π−alkyl)	
compound B[c] (allosteric inhibitor)	−10.85	3	Phe280, Lys279, Glu276		Phe280 (π−alkyl, $\pi-\pi$ stacked, and $\pi-\pi$ T-shaped), Leu192 ($\pi-\delta$ and π−alkyl), Phe196 ($\pi-\pi$ stacked and π−alkyl), Ile281 (alkyl)	

[a]Estimated binding free energy of the ligand−receptor complex. [b]The number of hydrogen bonds and all amino acid residues from the enzyme−inhibitor complex were determined with the AutoDock 4.2 program. [c]3-(3,5-Dibromo-4-hydroxy-benzoyl)-2-ethyl-benzofuran-6-sulfonic acid (4-sulfamoyl-phenyl)-amide.

strong hydrogen bond interactions via the hydroxy groups at positions 4, 13, and 13′ of compound **2a** with Glu276, Asn193, and Asp236 residues (Figure 3B). In addition, **2a** shared the same allosteric residues, including Leu192 (in the α3 helix) and Phe280 (in the α7 helix), with the reference allosteric inhibitor (compound B) via hydrophobic interactions. Similarly, at the allosteric site, the hydroxy groups at positions 10′, 11′, 10, and 4 of compound **3a** showed four hydrogen-bonding interactions with three residues (Asn193, Ala189, and Ser187) in the α3 helix of PTP1B (Figure 3D), with −9.35 kcal/mol binding energy. Interestingly, hydrophobic interactions were observed between ring B of both **2a** and **3a** and the allosteric residues Phe280 and Leu192. In addition, the benzene rings D of **3a** interacted with Glu276 via π−anion electrostatic interaction and Pro188 and Ala189 residues via hydrophobic interactions. A van der Waals interaction was also viewed between compound **3a** and the Gly277 residue in the α6 helix. These interactions were critical in blocking the interactions between α7 and α3−α6, preventing closure of the catalytic WPD loop and stabilizing PTP1B in an open, inactive conformation.[37] The negative binding energies of **2a** and **3a** indicated that they have a high affinity and tight binding capacity for the active site of PTP1B. These in silico results were concordant with the in vitro kinetic analysis results and demonstrated that the aglycone stilbene derivatives (**2a** and **3a**) are noncompetitive and allosteric PTP1B inhibitors.

EXPERIMENTAL SECTION

General Experimental Procedures. Optical rotations, IR, UV, NMR spectra, HRFABMS, HRESIMS, HPLC, and TLC, were carried out according to previously described procedures (Supporting Information).[38]

Plant Material. Roots from *P. multiflorum* were purchased from a traditional market in Jeonju-si, Korea, in January of 2018 and authenticated by one of the authors (B.S.M.). A voucher specimen (22A-PM) was stored at the Laboratory of Pharmacology in the College of Pharmacy, Kyungpook National University, Republic of Korea.

Extraction and Isolation. The dried roots of *P. multiflorum* (20.0 kg) were extracted and refluxed with 100% MeOH (9 L × 3) at 40 °C for 4 h. The extract was concentrated in vacuo to obtain a brown residue (2.44 kg). The residue was suspended in distilled water and successively partitioned with *n*-hexane, CH_2Cl_2, EtOAc, and *n*-butanol to afford *n*-hexane (80.1 g), CH_2Cl_2 (35.2 g), EtOAc (310.5 g), and *n*-butanol (308.7 g) fractions and an aqueous extract.

The EtOAc fraction (310.5 g) was chromatographed with vacuum liquid chromatography (VLC) on silica gel eluted with a CH_2Cl_2/MeOH gradient (2−100% MeOH) to yield four fractions: 52B−E. Fraction 52C (11.36 g) was subjected to column chromatography (CC) on MCI gel eluted with a MeOH/H_2O gradient (20−100% MeOH) to obtain 12 fractions: 53A−L. Fraction 53D (2.91 g) was separated on silica gel CC (CH_2Cl_2/MeOH/formic acid, 20:1:0.5 → 10:10:0.5) to obtain seven fractions: 56A−G. Fraction 56F (1.33 g) was chromatographed on MCI gel CC eluted with a mixture of MeOH/H_2O (40−100% MeOH) to obtain **8** (873.6 mg) and **6** (15.2 mg). Fraction 53E (318.5 mg) was chromatographed on a Sephadex LH-20 column using a gradient solvent system of MeOH/H_2O (50−100% MeOH) and yielded six fractions: 54A−F. Compounds **4** (4.0 mg, t_R = 32.0 min) and **10** (7.2 mg, t_R = 37.0 min) were obtained from fraction 54D (28.7 mg) by preparative HPLC (isocratic eluent, 45% MeOH in H_2O, 6 mL/min, 45 min). Fraction 54E (35.6 mg) was rechromatographed by preparative HPLC with an isocratic eluent (55% MeOH in H_2O, 6 mL/min, 30 min) to obtain **14** (10.7 mg, t_R = 18.0 min) and **15** (7.2 mg, t_R = 20.0 min). Fraction 53G (948.4 mg) was chromatographed on MCI gel CC eluted with a MeOH/H_2O gradient (55−100% MeOH) to obtain five fractions: 60A−E. Compound **12** (30.6 mg) was purified from fraction 60D with Sephadex LH-20 CC eluted with a mixture of MeOH/H_2O (1:1). Fraction 60E was passed over a Sephadex LH-20 column eluted with MeOH−H_2O (50%) to obtain **13** (31.8 mg) and fraction 60E3. Compound **7** (3.1 mg, t_R = 53.0 min) was obtained from fraction 60E3 by preparative HPLC with a MeOH/H_2O gradient (40−60% MeOH, 6 mL/min, 60 min). Fraction 53H (330.9 mg) was fractionated on a Sephadex LH-20 column (MeOH/H_2O, 1:1) to obtain **5** (20.8 mg) and fractions 66A−D. Compound **16** (8.1 mg, t_R = 20.5 min) was obtained from fraction 66B (30.6 mg) by preparative HPLC (isocratic eluent, 60% MeOH in H_2O, 6 mL/min, 35 min). Fraction 52D (183.2 g) was separated on silica gel VLC eluted with a CH_2Cl_2/MeOH/H_2O gradient (9:1:0.1 → 7:3:0.3) to obtain four fractions: 67A−D. Fraction 67D (10.2 g) was subjected to MCI gel CC eluted with a MeOH/H_2O gradient (20−100% MeOH) to obtain 12 fractions: 67D1−12. Fraction 67D9 (314.2 mg) was further chromatographed with preparative HPLC (isocratic eluent, 45% MeOH in H_2O, 6 mL/min, 40 min) to obtain **2** (70.5 mg, t_R = 27.0 min) and **3** (57.9 mg, t_R = 32.0 min). Compound **11** (30.1 mg, t_R = 16.5 min) was obtained from fraction 67D6 (94.1 mg) by preparative HPLC with an isocratic eluent of MeOH/H_2O (45% MeOH, 6 mL/min, 25 min). Fraction 67D7 (4.4 g) was separated on silica gel CC (CH_2Cl_2/MeOH/H_2O, 6.5:1:0.1) to obtain three fractions: 69A−C. Fraction 69C (256.2 mg) was further subjected to preparative HPLC (isocratic eluent, 40% MeOH in H_2O, 6 mL/min, 30 min) to obtain **1** (7.4 mg, t_R = 19.0 min) and **9** (7.1 mg, t_R = 21.5 min).

Polygonibene A (1). Brown powder; $[\alpha]_D^{21.2}$ + 81.0 (*c* 0.1, MeOH); UV (MeOH) λ_{max} (log ε) 235 (4.27), 310 (4.17) nm; IR (ATR) ν_{max} 3322, 1610, 1580, 1510, 1320, 1250, 1088 cm^{-1}; ECD (MeOH) λ_{max}

https://dx.doi.org/10.1021/acs.jnatprod.9b00777
J. Nat. Prod. XXXX, XXX, XXX−XXX

($\Delta\varepsilon$) 198 (−0.48), 212 (−1.06), 239 (+4.90) nm); ^{1}H NMR (methanol-d_4, 500 MHz) and ^{13}C NMR (methanol-d_4, 125 MHz), see Table 1; HRFABMS m/z 833.2271 [M + Na]$^+$ (calcd for $C_{40}H_{42}O_{18}Na$, 833.2269).

Polygonibene B (**2**). Brown powder; $[\alpha]_D^{21.2}$ + 99.8 (c 0.18, MeOH); UV (MeOH) λ_{max} (log ε) 230 (4.60), 325 (4.46) nm; ECD (MeOH) λ_{max} ($\Delta\varepsilon$) 204 (+2.48), 221 (−0.22), 239 (+0.48) nm; IR (ATR) ν_{max} 3340, 1620, 1590, 1512, 1330, 1250, 1096 cm^{-1}; ^{1}H NMR (methanol-d_4, 500 MHz) and ^{13}C NMR (methanol-d_4, 125 MHz), see Table 1; HRFABMS m/z 833.2273 [M + Na]$^+$ (calcd for $C_{40}H_{42}O_{18}Na$, 833.2269).

Polygonibene C (**3**). Brown powder; $[\alpha]_D^{21.2}$ −55.5 (c 0.13, MeOH); UV (MeOH) λ_{max} (log ε) 230 (4.55), 320 (4.40) nm; ECD (MeOH) λ_{max} ($\Delta\varepsilon$) 205 (−1.32), 218 (+0.58), 236 (−0.61) nm; IR (ATR) ν_{max} 3328, 1620, 1590, 1510, 1330, 1250, 1098 cm^{-1}; ^{1}H NMR (methanol-d_4, 500 MHz) and ^{13}C NMR (methanol-d_4, 125 MHz), see Table 1; HRFABMS m/z 833.2272 [M + Na]$^+$ (calcd for $C_{40}H_{42}O_{18}Na$, 833.2269).

Polygonibene D (**4**). Brown powder; $[\alpha]_D^{21.2}$ +27.7 (c 0.03, MeOH); UV (MeOH) λ_{max} (log ε) 235 (3.45), 310 (3.54) nm; IR (ATR) ν_{max} 3326, 1739, 1620, 1580, 1510, 1320, 1260, 1088 cm^{-1}; ^{1}H NMR (acetone-d_6, 500 MHz) and ^{13}C NMR (acetone-d_6, 125 MHz), see Table 2; HRESIMS m/z 449.1445 [M + H]$^+$ (calcd for $C_{21}H_{25}O_{10}$, 449.1458).

Polygonibene E (**5**). Brown powder; $[\alpha]_D^{21.2}$ −12.8 (c 0.2, MeOH); UV (MeOH) λ_{max} (log ε) 225 (4.45), 325 (4.45) nm; IR (ATR) ν_{max} 3316, 1740, 1620, 1570, 1512, 1330, 1260, 1140 cm^{-1}; ^{1}H NMR (acetone-d_6, 500 MHz) and ^{13}C NMR (acetone-d_6, 125 MHz), see Table 2; HRESIMS m/z 605.1636 [M + Na]$^+$ (calcd for $C_{30}H_{30}O_{12}Na$, 605.1635).

Polygonibene F (**6**). Brown powder; $[\alpha]_D^{21.2}$+25.2 (c 0.2, MeOH); UV (MeOH) λ_{max} (log ε) 225 (4.23), 325 (4.35) nm; IR (ATR) ν_{max} 3327, 1740, 1620, 1580, 1510, 1330, 1260, 1150 cm^{-1}; ^{1}H NMR (acetone-d_6, 500 MHz) and ^{13}C NMR (acetone-d_6, 125 MHz), see Table 2; HRFABMS m/z 435.1288 [M + H]$^+$ (calcd for $C_{21}H_{23}O_{10}$, 435.1291).

Polygonibene G (**7**). Brown powder; $[\alpha]_D^{21.2}$ −46.3 (c 0.04, MeOH); UV (MeOH) λ_{max} (log ε) 230 (3.98), 290 (3.99) nm; ECD (MeOH) λ_{max} ($\Delta\varepsilon$) 207 (−1.64), 229 (+4.61), 250 (−1.30) nm; IR (ATR) ν_{max} 3397, 1741, 1620, 1570, 1510, 1330, 1260, 1088 cm^{-1}; ^{1}H NMR (methanol-d_4, 500 MHz) and ^{13}C NMR (methanol-d_4, 125 MHz), see Table 2; HRESIMS m/z 605.1631 [M + Na]$^+$ (calcd for $C_{30}H_{30}O_{12}Na$, 605.1635).

(E)-2,3,5,4′-Tetrahydroxystilbene-2-O-α-L-rhamnoside (**15**). Brown powder; ^{1}H NMR (acetone-d_6, 500 MHz) δ_H 7.74 (1H, d, J = 16.5 Hz, H-α), 7.41 (2H, d, J = 8.6 Hz, H-2′,6′), 6.92 (1H, d, J = 16.5 Hz, H-β), 6.78 (2H, d, J = 8.6 Hz, H-3′,5′), 6.63 (1H, d, J = 2.8 Hz, H-6), 6.24 (1H, d, J = 2.8 Hz, H-4), 4.47 (1H, d, J = 7.9 Hz, H-1″), 3.57 (1H, t, J = 8.5 Hz, H-3″), 3.42 (1H, m, H-2″), 3.38 (1H, m, H-5″), 3.14 (1H, td, J = 4.5, 9.1 Hz, H-4″), 1.27 (3H, d, J = 6.1 Hz, H-6″); ^{13}C NMR (acetone-d_6, 125 MHz) δ_C 158.1 (C-4′), 155.8 (C-5), 152.1 (C-3), 137.9 (C-2), 133.3 (C-1), 130.5 (C-1′), 129.3 (C-β), 128.9 (C-2′,6′), 121.9 (C-α), 116.3 (C-3′,5′), 107.6 (C-1″), 103.5 (C-4), 102.1 (C-6), 77.7 (C-2″), 76.3 (C-4″), 75.6 (C-3″), 73.5 (C-5″), 18.1 (C-6″). HRESIMS m/z 413.1208 [M + Na]$^+$ (calcd for $C_{20}H_{22}O_8Na$, 413.1212).

Acid Hydrolysis of 2, 3, and 8. Compounds **2**, **3**, and **8** (30 mg each) were individually refluxed with 10% HCl (10 mL) for 3 h at 90 °C, and each reaction mixture was extracted with EtOAc. After the aqueous layer was neutralized with $BaCO_3$, the precipitates were filtered, and the filtrate was repeatedly evaporated in vacuo to yield a colorless syrup that was purified by preparative TLC (solvent $CHCl_3$/MeOH/H_2O 8:5:1) (R_f 0.31). According to a previously reported method,[39] the monosaccharide residue was identified as D-glucose. Each EtOAc layer was washed with aqueous 5% $NaHCO_3$, dried, and evaporated to yield a brown powder. The resultant residue was purified by preparative HPLC using MeOH/H_2O elution (45% MeOH, 6 mL/min, 40 min) to obtain the respective deglucosylated stilbenes **8a** (5.2 mg, t_R = 25.0 min),[18] **2a** (1.1 mg, t_R = 27.5 min), and **3a** (1.2 mg, t_R = 29.5 min). Their structures were confirmed by HRESIMS, ^{1}H NMR, ECD spectra, and optical rotation data.

(E)-2,3,5,4′-Tetrahydroxystilbene (**8a**). Brown powder; ^{1}H NMR (acetone-d_6, 500 MHz) δ_H 7.39 (2H, d, J = 8.5 Hz, H-2′,6′), 7.29 (1H, d, J = 16.5 Hz, H-β), 7.01 (1H, d, J = 16.5 Hz, H-α), 6.83 (2H, d, J = 8.5 Hz, H-3′,5′), 6.56 (1H, d, J = 2.6 Hz, H-6), 6.34 (1H, t, J = 2.6 Hz, H-4); HRESIMS m/z 245.0829 [M + H]$^+$ (calcd for $C_{14}H_{13}O_4$, 245.0814).

10,10′-Deglucosyl-polygonibene B (**2a**). Brown powder; $[\alpha]_D^{21.2}$ +34.5 (c 0.02, MeOH); ECD (MeOH) 200 nm ($\Delta\varepsilon$ + 1.18), 222 nm ($\Delta\varepsilon$ + 0.07), 240 nm ($\Delta\varepsilon$ + 0.95); ^{1}H NMR (methanol-d_4, 500 MHz) δ_H 7.35 (1H, dd, J = 8.3, 1.8 Hz, H-6′), 7.25 (2H, d, J = 8.5 Hz, H-2,6), 7.23 (1H, d, J = 16.4 Hz, H-8′), 7.22 (1H, d, J = 1.8 Hz, H-2′), 6.97 (1H, d, J = 16.4 Hz, H-7′), 6.85 (1H, d, J = 8.3 Hz, H-5′), 6.75 (2H, d, J = 8.5 Hz, H-3,5), 6.47 (1H, d, J = 2.7 Hz, H-14′), 6.27 (1H, d, J = 2.8 Hz, H-12), 6.23 (1H, d, J = 2.7 Hz, H-12′), 5.94 (1H, d, J = 2.8 Hz, H-14), 5.55 (1H, d, J = 6.6 Hz, H-7), 4.93 (1H, d, J = 6.6 Hz, H-8); HRESIMS m/z 487.1398 [M + H]$^+$ (calcd for $C_{28}H_{23}O_8$, 487.1392).

10,10′-Deglucosyl-polygonibene C (**3a**). Brown powder; $[\alpha]_D^{21.2}$ −11.2 (c 0.02, MeOH), ECD (MeOH) 209 nm ($\Delta\varepsilon$ + 2.76), 239 nm ($\Delta\varepsilon$ −3.35); ^{1}H NMR (methanol-d_4, 500 MHz) δ_H 7.35 (1H, dd, J = 8.3, 1.7 Hz, H-6′), 7.26 (2H, d, J = 8.5 Hz, H-2,6), 7.23 (1H, d, J = 16.4 Hz, H-8′), 7.22 (1H, d, J = 1.7 Hz, H-2′), 6.98 (1H, d, J = 16.4 Hz, H-7′), 6.85 (1H, d, J = 8.3 Hz, H-5′), 6.75 (2H, d, J = 8.5 Hz, H-3,5), 6.48 (1H, d, J = 2.8 Hz, H-14′), 6.28 (1H, d, J = 2.8 Hz, H-12), 6.24 (1H, d, J = 2.8 Hz, H-12′), 5.95 (1H, d, J = 2.8 Hz, H-14), 5.56 (1H, d, J = 6.6 Hz, H-7), 4.94 (1H, d, J = 6.6 Hz, H-8); HRESIMS m/z 487.1397 [M + H]$^+$ (calcd for $C_{28}H_{23}O_8$, 487.1392).

PTP1B Inhibitory Assay. The PTP1B inhibitory activity of compounds **1**−**16**, **2a**, **3a**, and **8a** were evaluated using p-nitrophenyl phosphate (p-NPP) as a substrate and ursolic acid as a positive control according to a previously reported procedure.[40] IC_{50} values were calculated using nonlinear regression analysis in an Excel (Microsoft Excel 2016, U.S.A.) spreadsheet.

PTP1B Kinetic Assay. The PTP1B kinetic analysis was conducted using the method previously described by Tuan et al. (Supporting Information).[40]

Molecular Docking Simulation. The docking protocol was carried out with the AutoDock 4.2 program using a previously described method[40] with modifications (Supporting Information).

Statistical Analysis. Statistical analyses were performed as previously described (Supporting Information).[40]

■ ASSOCIATED CONTENT

Supporting Information

The Supporting Information is available free of charge at https://pubs.acs.org/doi/10.1021/acs.jnatprod.9b00777.

Experimental methods, 1D and 2D NMR and HRMS spectra of polygonibenes A−G (**1**−**7**) and ^{1}H NMR spectra of compounds **2a** and **3a**, ECD spectra of compounds **1**, **2a**, **3a**, ε-viniferin, and δ-viniferin, and kinetic studies for selected compounds **2a** and **3a** (PDF)

■ AUTHOR INFORMATION

Corresponding Authors

Byung Sun Min − *Daegu Catholic University, Gyeongbuk, Republic of Korea*; Phone: +82-850-3613; Email: bsmin@cu.ac.kr; Fax: +82-53-850-3602

Jeong Ah Kim − *Kyungpook National University, Daegu, Republic of Korea*; orcid.org/0000-0001-7337-1812; Phone: +82-53-950-8574; Email: jkim6923@knu.ac.kr; Fax: +82-53-950-8557

https://dx.doi.org/10.1021/acs.jnatprod.9b00777
J. Nat. Prod. XXXX, XXX, XXX−XXX

Other Authors

Thi-Thuy An Nguyen − *Kyungpook National University, Daegu, Republic of Korea*

Manh Tuan Ha − *Daegu Catholic University, Gyeongbuk, Republic of Korea*

Se-Eun Park − *Pukyong National University, Busan, Republic of Korea*

Jae Sue Choi − *Pukyong National University, Busan, Republic of Korea;* orcid.org/0000-0001-9034-8868

Complete contact information is available at: https://pubs.acs.org/10.1021/acs.jnatprod.9b00777

Author Contributions

⊥T.T.A.N. and M.T.H. contributed equally to this article.

Notes

The authors declare no competing financial interest.

■ ACKNOWLEDGMENTS

This research was supported by the National Research Foundation of Korea (NRF), funded by the Ministry of Science, ICT, and Future Planning (NRF-2018R1D1A1B07045287), and a grant (18182MFDS214) from Ministry of Food and Drug Safety in 2018. We are grateful to the Korea Basic Science Institute (KBSI) for mass spectrometric measurements.

■ REFERENCES

(1) Zhang, S.; Zhang, Z. Y. *Drug Discovery Today* **2007**, *12*, 373−381.
(2) Johnson, T. O.; Ermolieff, J.; Jirousek, M. R. *Nat. Rev. Drug Discovery* **2002**, *1*, 696−709.
(3) Elchebly, M.; Payette, P.; Michaliszyn, E.; Cromlish, W.; Collins, S.; Loy, A. L.; Normandin, D.; Cheng, A.; Himms-Hagen, J.; Chan, C. C.; Ramachandran, C.; Gresser, M. J.; Tremblay, M. L.; Kennedy, B. P. *Science* **1999**, *283*, 1544−1548.
(4) Klaman, L. D.; Boss, O.; Peroni, O. D.; Kim, J. K.; Martino, J. L.; Zabolotny, J. M.; Moghal, N.; Lubkin, M.; Kim, Y. B.; Sharpe, A. H.; Stricker-Krongrad, A.; Shulman, G. I.; Neel, B. G.; Kahn, B. B. *Mol. Cell. Biol.* **2000**, *20*, 5479−5489.
(5) Yip, S. C.; Saha, S.; Chernoff, J. *Trends Biochem. Sci.* **2010**, *35*, 442−449.
(6) Bentires-Alj, M.; Neel, B. G. *Cancer Res.* **2007**, *67*, 2420−2424.
(7) Stuible, M.; Doody, K. M.; Tremblay, M. L. *Cancer Metastasis Rev.* **2008**, *27*, 215−230.
(8) Julien, S. G.; Dubé, N.; Read, M.; Penney, J.; Paquet, M.; Han, Y.; Kennedy, B. P.; Muller, W. J.; Tremblay, M. L. *Nat. Genet.* **2007**, *39*, 338.
(9) Través, P. G.; Pardo, V.; Pimentel-Santillana, M.; González-Rodríguez, Á.; Mojena, M.; Rico, D.; Montenegro, Y.; Cales, C.; Martin-Sanz, P.; Valverde, A. M.; Boscá, L. *Cell Death Dis.* **2014**, *5*, No. e1125.
(10) Vieira, M. N.; Lyra e Silva, N. M.; Ferreira, S. T.; De Felice, F. G. *Front. Aging Neurosci.* **2017**, *9*, 7.
(11) Tautz, L. *J. Clin. Invest.* **2015**, *125*, 2931−2934.
(12) Jeong, B.; Choi, S. Y.; Jang, H. S.; Yoo, G.; Kim, S. H.; Kim, J. H.; Kwon, Y. S.; Roh, J. S.; Yoon, Y.; Shin, S. S.; Yang, H. *Nat. Prod. Sci.* **2017**, *23*, 9−15.
(13) Jiang, C. S.; Liang, L. F.; Guo, Y. W. *Acta Pharmacol. Sin.* **2012**, *33*, 1217.
(14) Ha, M. T.; Park, D. H.; Shrestha, S.; Kim, M.; Kim, J. A.; Woo, M. H.; Choi, J. S.; Min, B. S. *Fitoterapia* **2018**, *131*, 119−126.
(15) Shen, T.; Wang, X. N.; Lou, H. X. *Nat. Prod. Rep.* **2009**, *26*, 916−935.
(16) Lv, G.; Lou, Z.; Chen, S.; Gu, H.; Shan, L. *J. Ethnopharmacol.* **2011**, *137*, 449−456.
(17) Lv, L.; Gu, X.; Tang, J.; Ho, C. T. *Food Chem.* **2007**, *104*, 1678−1681.
(18) Ryu, G.; Ju, J. H.; Park, Y. J.; Ryu, S. Y.; Choi, B. W.; Lee, B. H. *Arch. Pharmacal Res.* **2002**, *25*, 636−639.
(19) Wang, X.; Zhao, L.; Han, T.; Chen, S.; Wang, J. *Eur. J. Pharmacol.* **2008**, *578*, 339−348.
(20) Yao, W.; Fan, W.; Huang, C.; Zhong, H.; Chen, X.; Zhang, W. *Biomed. Pharmacother.* **2013**, *67*, 140−145.
(21) Kim, H. K.; Choi, Y. H.; Choi, J. S.; Choi, S. U.; Kim, Y. S.; Lee, K. R.; Kim, Y.-K.; Ryu, S. Y. *Arch. Pharmacal Res.* **2008**, *31*, 1225.
(22) Hoang, D. M.; Trung, T. N.; Hien, P. T. T.; Ha, D. T.; Van Luong, H.; Lee, M.; Bae, K. *Nat. Prod. Sci.* **2010**, *16*, 239−244.
(23) Ngoc, T. M.; Minh, P. T. H.; Hung, T. M.; Thuong, P. T.; Lee, I.; Min, B. S.; Bae, K. *Arch. Pharmacal Res.* **2008**, *31*, 598.
(24) Lemière, G.; Gao, M.; De Groot, A.; Dommisse, R.; Lepoivre, J.; Pieters, L.; Buss, V. *J. Chem. Soc., Perkin Trans. 1* **1995**, 1775−1779.
(25) Ito, T.; Masuda, Y.; Abe, N.; Oyama, M.; Sawa, R.; Takahashi, Y.; Chelladurai, V.; Iinuma, M. *Chem. Pharm. Bull.* **2010**, *58*, 1369−1378.
(26) Timperio, A. M.; D'Alessandro, A.; Fagioni, M.; Magro, P.; Zolla, L. *Plant Physiol. Biochem.* **2012**, *50*, 65−71.
(27) Kumar, S.; Lee, H. Y.; Liou, J. P. *J. Nat. Prod.* **2017**, *80*, 1294−1301.
(28) Chen, W. S.; Zhang, W. D.; Yang, G. J.; Chen, H. S.; Qiao, C. Z. *Chin. Chem. Lett.* **2001**, *12*, 503−506.
(29) Brecker, L.; Mahut, M.; Schwarz, A.; Nidetzky, B. *Magn. Reson. Chem.* **2009**, *47*, 328−332.
(30) Li, X. M.; Lin, M.; Wang, Y. H.; Liu, X. *Planta Med.* **2004**, *70*, 160−165.
(31) Wungsintaweekul, B.; Umehara, K.; Miyase, T.; Noguchi, H. *Phytochemistry* **2011**, *72*, 495−502.
(32) Fan, W.; Tezuka, Y.; Xiong, Q.; Hattori, M.; Namba, T.; Kadota, S. *Chem. Pharm. Bull.* **1999**, *47*, 1049−1050.
(33) Pozdeeva, A. V.; Komarova, N. I.; Vasiliev, V. G.; Rogachev, A. D.; Salakhutdinov, N. F.; Tolstikov, G. A. *Mendeleev Commun.* **2013**, *23*, 37−38.
(34) Mannila, E.; Talvitie, A.; Kolehmainen, E. *Phytochemistry* **1993**, *33*, 813−816.
(35) Sun, Y. N.; Cui, L.; Li, W.; Yan, X. T.; Yang, S. Y.; Kang, J. I.; Kang, H. K.; Kim, Y. H. *Bioorg. Med. Chem. Lett.* **2013**, *23*, 4801−4805.
(36) Li, X. C.; Liu, C.; Yang, L. X.; Chen, R. Y. *J. Asian Nat. Prod. Res.* **2011**, *13*, 826−830.
(37) Wiesmann, C.; Barr, K. J.; Kung, J.; Zhu, J.; Erlanson, D. A.; Shen, W.; Fahr, B. J.; Zhong, M.; Taylor, L.; Randal, M.; McDowell, R. S.; Hansen, S. K. *Nat. Struct. Mol. Biol.* **2004**, *11*, 730.
(38) Pham, V. C.; Nguyen, T. T. A.; Vu, T. O.; Cao, T. Q.; Min, B. S.; Kim, J. A. *Phytochem. Lett.* **2019**, *32*, 23−28.
(39) Ngo, Q. M. T.; Lee, H. S.; Nguyen, V. T.; Kim, J. A.; Woo, M. H.; Min, B. S. *Phytochemistry* **2017**, *141*, 147−155.
(40) Ha, M. T.; Seong, S. H.; Nguyen, T. D.; Cho, W. K.; Ah, K. J.; Ma, J. Y.; Woo, M. H.; Choi, J. S.; Min, B. S. *Phytochemistry* **2018**, *155*, 114−125.